

1 **Supplementary Information**

2 **Novel naturally-derived encapsulation agents in the**  
3 **ionic liquid form for sustainable emulsion-based**  
4 **products**

5 *Ariel A. C. Toledo Hijo<sup>a,\*</sup>, Eric Keven Silva<sup>a</sup>, Aureliano A. D. Meirelles<sup>a</sup>, Rosiane L. Cunha<sup>a</sup>,*  
6 *Antonio J. A. Meirelles<sup>a,\*</sup>*

7  
8 <sup>a</sup> School of Food Engineering, University of Campinas, R. Monteiro Lobato 80, 13083-862,  
9 Campinas, São Paulo, Brazil

10 \*Correspondence: tomze@unicamp.br Tel.: +55 19 3521 4056 (A.J.A.M.);

11 arieltolledohijo@gmail.com (A.A.C.T.H.)

## 19 **Material and methods**

### 20 **Materials**

21 Materials used for ILs synthesis were diethanolamine (H<sub>2</sub>EA, bis(2-hydroxyethyl)amine),  
22 stearic (C<sub>18</sub>OOH) and oleic (C<sub>18:1</sub>OOH) acids (Sigma-Aldrich, St. Louis, purity > 99% w/w) and  
23 choline (Ch) hydroxide (Sigma-Aldrich, St. Louis, aqueous solution, 46% w/w). The specific FAs  
24 were chosen to evaluate the effect of the unsaturation on the emulsion encapsulation, taking into  
25 account their significance in the FA profile of the main edible vegetable oils. Deionized water was  
26 used as emulsions' aqueous phase and tunisian rosemary (*Rosmarinus officinalis*) essential oil  
27 (Ferquima Ind. e Com. Ltda, Vargem Grande Paulista, Brazil) as core material. Aqueous choline  
28 hydroxide was chosen instead of the methanol-based one, considering the application potential of  
29 choline-based ILs in the food industry and the toxicity concerns associated to methanol.

### 30 **Synthesis of the ILs and characterization**

31 Diethanolammonium stearate ([H<sub>2</sub>EA][C<sub>18</sub>OO]) and diethanolammonium oleate  
32 ([H<sub>2</sub>EA][C<sub>18:1</sub>OO]) were synthesized through the Brønsted acid-base reaction between the FA and  
33 diethanolamine at  $x_1 = 0.5$ . The synthesis was performed in a nitrogen atmosphere at temperatures  
34 above the mesophase domain and cooled down to room temperature. Cholinium stearate  
35 ([Ch][C<sub>18</sub>OO]) was synthesized through the acid-base reaction between stearic acid dissolved in  
36 ethanol solution and choline hydroxide at  $x_1 = 0.5$ . The synthesis was performed in a thermal fluid  
37 bath at room temperature and in a nitrogen atmosphere to avoid the oxidation of the compounds.  
38 The reaction resulted in IL aqueous-ethanolic solutions, which were dried under vacuum at 50 °C  
39 for 24 hours to obtain a white powder emulsifier. Their water content was determined by Karl  
40 Fisher titration, obtaining values lower than 1.5%. ILs were characterized by proton Nuclear

41 Magnetic Resonance ( $^1\text{H}$  NMR) by using a Bruker 300 Fourier 300 MHz and Attenuated Total  
42 Reflectance-Fourier Transform Infrared spectroscopy (ATR-FTIR ALPHA, Bruker Scientific,  
43 Banner Lane). The structures of ILs and the effectiveness of the synthesis were confirmed by the  
44 spectra.

#### 45 **Emulsion preparation**

46 Emulsions were prepared by pre-mixing using Ultra Turrax (U) followed by high-intensity  
47 ultrasound-assisted encapsulation process (HIUS) using ILs ( $[\text{H}_2\text{EA}][\text{C}_{18}\text{OO}]$ ,  $[\text{H}_2\text{EA}][\text{C}_{18:1}\text{OO}]$   
48 or  $[\text{Ch}][\text{C}_{18}\text{OO}]$ ) at a fixed concentration (1.0%, w/w). Rosemary essential oil was used as oily  
49 phase at 1.0% (w/w). Emulsions were prepared at room temperature ( $\pm 25$  °C) by pre-mixing the  
50 aqueous and oily phases using a U model T18 (IKA, Staufen, Germany). Previously, IL was  
51 dissolved into the water. The essential oil was added dropwise at 5.000 rpm for 5 min. Then, the  
52 pre-mixing condition was fixed at 10.000 rpm for 20 min for a 40 g sample, resulting in a specific  
53 energy of 6000 J/g obtained according to Eq. 1. After pre-mixing, the system was submitted to  
54 ultrasound treatment using an ultrasonic probe (13 mm of diameter) (Unique, Desruptor, 800 W,  
55 Indaiatuba, Brazil) at 720 W for 4.65 min for a 40 g sample, resulting in a specific energy of 5022  
56 J/g (Eq. 1), totalizing 11022 J/g for both processes. A refrigerated bath at 5 °C was used to avoid  
57 excessive heating in all samples submitted to HIUS processing.

$$58 \quad \text{Specific energy} \left( \frac{\text{J}}{\text{g}} \right) = \frac{\text{Nominal power (W)} \times \text{Time (s)}}{\text{Weight (g)}} \quad (1)$$

59 The acoustic power provided by the ultrasound probe for the nominal power of 720 W was  
60 determined by calorimetric assays according to a methodology previously described<sup>1</sup>. The HIUS  
61 intensity was calculated from the acoustic power according to Eq. 2:

$$62 \quad \text{HIUS intensity} \left( \frac{\text{W}}{\text{cm}^2} \right) = \frac{4 \times \text{acoustic power}}{\pi D^2} \quad (2)$$

63 where D (cm) is the probe diameter.

64 The HIUS intensity was 20 W/cm<sup>2</sup> for the nominal power of 720 W.

65 Trials were named according to the IL.

## 66 **Kinetic stability**

67 The visual aspect and kinetic stability of the emulsions were evaluated in cylindrical glass  
68 tubes (2.23 cm internal diameter and 12.81 cm height), properly sealed, and stored for 30 days at  
69 25 °C. After preparation, 20 mL of each emulsion were immediately transferred to a glass tube.  
70 The oil phase separation was measured and may be expressed as the ratio between the height of  
71 the superior phase (H<sub>S</sub>) and the total height of the emulsion (H<sub>T</sub>), as shown in Eq. (3). The  
72 measurements were performed in duplicate at least.

$$73 \quad \text{Emulsion Stability (\%)} = \frac{H_S}{H_T} \times 100 \quad (3)$$

74 The emulsion stability was also evaluated and confirmed using an optical scanning device  
75 Turbiscan LAB Expert (Formulacion, France), using the same sample that was placed in a  
76 cylindrical glass measurement cell (2.23 cm internal diameter and 12.81 cm height) and stored for  
77 30 days. The backscattering (% BS) of monochromatic light ( $\lambda = 880$  nm) was measured as a  
78 function of the emulsion height at 25 °C. The backscattering profile (BS versus emulsion height)  
79 of each emulsion was measured after 1, 2, 7, 14 and 30 days of storage time.

80

81

82

### 83 **Optical microscopy**

84 The microstructure of the emulsions was characterized after 1 and 7 days of storage using an  
85 optical microscope (Leica, Cambridge, UK). An emulsion droplet was put in slides with coverslips  
86 and observed with  $\times 40$  and  $\times 100$  objective lenses. The measurements were performed in triplicate  
87 at least.

### 88 **Rheological assays**

89 The rheological behavior and the viscosity profile of the emulsions were determined after 1  
90 and 7 days of storage using an AR 1500ex stress controlled rotational rheometer (TA Instruments,  
91 New Castle, DE). Flow curves were obtained in an up-down-up step program at 25 °C, in which  
92 the shear rate ranged from 0 to 300 s<sup>-1</sup>, using a stainless steel cone and plate (diameter = 40 mm,  
93 angle = 2° and cone truncation = 57 μm). In order to characterize the steady-state behavior of the  
94 shear stress ( $\sigma$ ) – shear rate ( $\dot{\gamma}$ ) profile of the emulsions, the results were obtained at the third step  
95 program. The measurements were performed in triplicate at least.

96 Flow curves were fitted to the Herschel-Bulkley (HB) model to obtain the rheological  
97 parameters according to Eq. (4).

$$98 \quad \sigma = \sigma_0 + k\dot{\gamma}^n \quad (4)$$

99 where  $\sigma$  is the shear stress (Pa),  $\dot{\gamma}$  is the shear rate (s<sup>-1</sup>);  $\sigma_0$  is the yield stress (Pa);  $k$  is the  
100 consistency index;  $n$  is the flow behavior index.

### 101 **Encapsulation Efficiency**

102 An aliquot of 0.5 mL of each sample was dissolved in 1.5 mL of ethyl acetate (Synth, lot  
103 153016, Diadema, Brazil) and manually homogenized. Then, the mixture was centrifuged at  
104 13,000 rpm for 10 min. Just after that, the samples were manually homogenized again and  
105 centrifuged at 13,000 rpm for 5 min. An aliquot of 1 mL of supernatant was filtered using nylon  
106 membrane (0.45  $\mu\text{m}$ ) and injected into the chromatograph. The sample split ration was 1:20. The  
107 carrier gas (Helium, 99.9% purity, White Martins, Campinas, Brazil) flowed at 1.1 mL/min. The  
108 injector and the detector temperatures were 220  $^{\circ}\text{C}$  and at 240  $^{\circ}\text{C}$ , respectively. The column was  
109 heated from 60  $^{\circ}\text{C}$  to 246  $^{\circ}\text{C}$  at 3  $^{\circ}\text{C}/\text{min}$ . A chromatograph GC-FID (Shimadzu, CG17A, Kyoto,  
110 Japan) equipped with a capillary column of fused silica DB-5 (J&W Scientific, 30 m  $\times$  0.25 mm  
111  $\times$  0.25  $\mu\text{m}$ , Folsom, USA) was used. The 1,8 cineole (Scheme S1) presented in emulsions was  
112 identified by comparing the retention indices of the samples and external standards. Quantification  
113 was performed using external standard calibration curves (Figure S1) and used to calculate the  
114 encapsulation efficiency of eucalyptol (1,8 cineole).

115 The encapsulation efficiency was measured and may be expressed as the ratio between the  
116 amount of bioactive effectively retained ( $Q_e$ ) and the initial amount added to the emulsion ( $Q_i$ ),  
117 according to Eq. (5).

$$118 \quad \text{Encapsulation Efficiency (\%)} = \frac{Q_e}{Q_i} \times 100 \quad (5)$$

### 119 **Statistical analysis**

120 The statistical analysis was performed using the software Statistica 7.0 (Statsoft Inc., Tulsa,  
121 USA). The significant differences ( $p < 0.05$ ) between the treatments and the comparison between  
122 the mean values were evaluated by the Tukey test.

123

124

## 125 RESULTS

### 126 ILs characterization by Fourier Transform Infrared spectroscopy (FT-IR)

127 The list of main IR spectroscopy bands for all ILs obtained by FT-IR is presented below:

#### 128 *diethanolammonium stearate ([H<sub>2</sub>EA][C<sub>18</sub>OO])*

129 IR (neat)  $\nu = 2915, 2849, 1550, 1465, 1406, 1069, 952, 721 \text{ cm}^{-1}$ .

#### 130 *diethanolammonium oleate ([H<sub>2</sub>EA][C<sub>18:1</sub>OO])*

131 IR (neat)  $\nu = 2923, 2851, 1556, 1456, 1402, 1071, 958, 722 \text{ cm}^{-1}$ .

#### 132 *cholinium stearate ([Ch][C<sub>18</sub>OO])*

133 IR (neat)  $\nu = 2914, 2848, 1569, 1467, 1388, 1092, 955, 718 \text{ cm}^{-1}$ .

134

### 135 ILs characterization by Proton Nuclear Magnetic Resonance (<sup>1</sup>H NMR)

136 The list of chemical shifts for all ILs obtained by <sup>1</sup>H NMR is presented below:

137

#### 138 *cholinium stearate ([Ch][C<sub>18</sub>OO])*

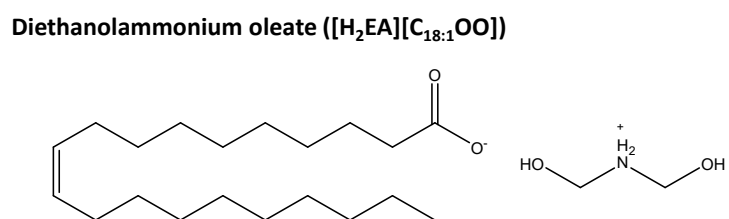
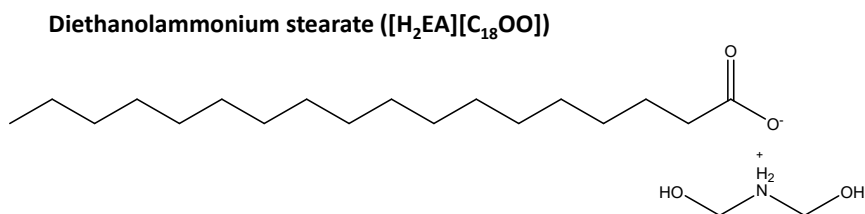
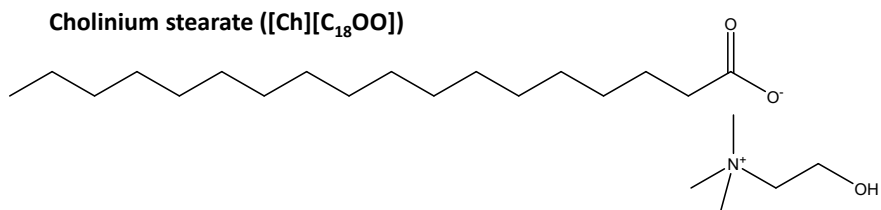
139 <sup>1</sup>H NMR (300 MHz, CDCl<sub>3</sub>)  $\delta$  ppm: 3.94 (m, 2H, -CH<sub>2</sub>-O), 3.49 (t, 2H, -CH<sub>2</sub>-), 3.17 (s, 9H, CH<sub>3</sub>-  
140 N), 2.03 (t, 2H, -CH<sub>2</sub>-COO<sup>-</sup>), 1.45 (m, 2H, -CH<sub>2</sub>-), 1.18 (m, 28H), 0.81 (t, 3H, CH<sub>3</sub>-).

#### 141 *diethanolammonium stearate ([H<sub>2</sub>EA][C<sub>18</sub>OO])*

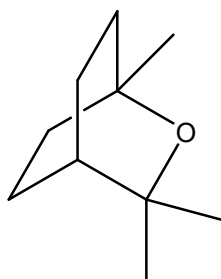
142 <sup>1</sup>H NMR (300 MHz, CDCl<sub>3</sub>)  $\delta$  ppm: 5.79 (s, 2H, -NH<sub>2</sub><sup>+</sup>), 3.77 (t, 2H, -CH<sub>2</sub>-O), 3.01 (t, 2H, -CH<sub>2</sub>-  
143 N), 2.09 (t, 2H, -CH<sub>2</sub>-COO<sup>-</sup>), 1.47 (m, 2H, -CH<sub>2</sub>-), 1.18 (m, 28H), 0.81 (t, 3H, CH<sub>3</sub>-).

#### 144 *diethanolammonium oleate ([H<sub>2</sub>EA][C<sub>18:1</sub>OO])*

145 <sup>1</sup>H NMR (300 MHz, CDCl<sub>3</sub>)  $\delta$  ppm: 5.29 (m, 3H, -NH<sub>2</sub><sup>+</sup>), 3.53 (t, 2H, -CH<sub>2</sub>-O), 2.75 (t, 2H, -CH<sub>2</sub>-  
146 N), 2.04 (t, 2H, -CH<sub>2</sub>-COO<sup>-</sup>), 1.96 (m, 6H), 1.44 (m, 2H, -CH<sub>2</sub>-), 1.22 (m, 20H), 0.84 (t, 3H, CH<sub>3</sub>-).



147

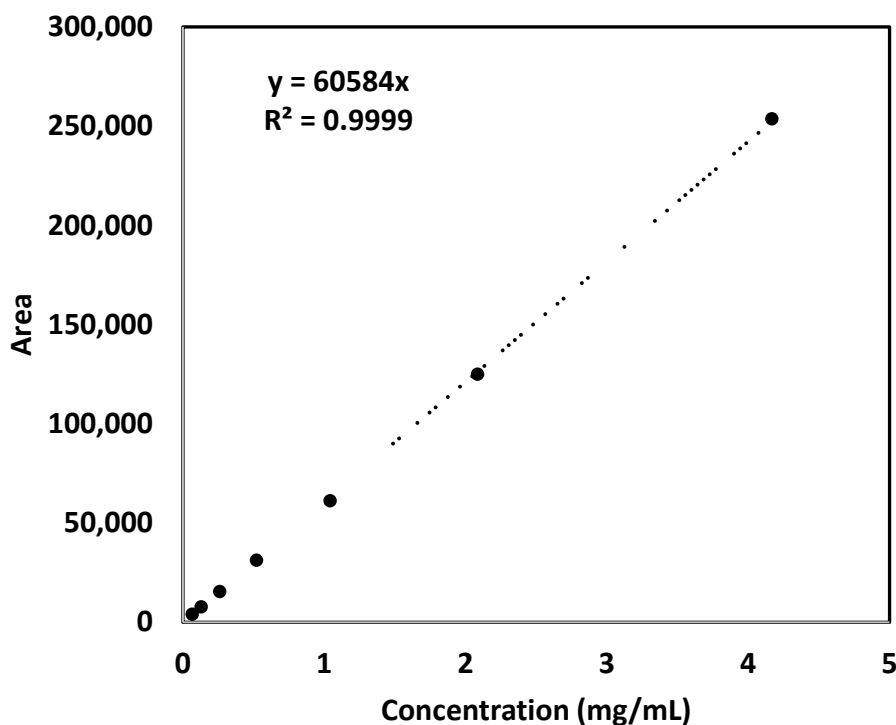


148

Eucalyptol

149 **Scheme S1.** Molecular structures of ILs and eucalyptol (1,8 cineole).





150

151 **Figure S1.** Standard calibration curve for eucalyptol.

152 **Table S1.** Rheological model parameters related to shear stress/shear rate curves fitted to flow  
 153 experimental data and apparent viscosity for IL emulsions. Different letters in samples in the same  
 154 day of storage, using different ILs, indicate significant difference at  $p < 0.05$ . Capital letters:  
 155 difference between storage time using the same IL.

Day 1					
IL	$\sigma_0/\text{Pa}$	$k^{\ddagger}$	$n^{\dagger}$	$R^2$	$\eta/\text{Pa}\cdot\text{s at } 100 \text{ s}^{-1}$
[H <sub>2</sub> EA][C <sub>18</sub> OO]	0.0	0.0064	0.78	0.9981	0.0035 ± 0.00027 aA
[H <sub>2</sub> EA][C <sub>18:1</sub> OO]	0.0	0.0011	1.00	0.9990	0.0019 ± 0.00007 bA
[Ch][C <sub>18</sub> OO]	0.0	0.0072	0.77	0.9987	0.0037 ± 0.00006 aA
Day 7					
IL	$\sigma_0/\text{Pa}$	$k^{\ddagger}$	$n^{\dagger}$	$R^2$	$\eta/\text{Pa}\cdot\text{s at } 100 \text{ s}^{-1}$
[H <sub>2</sub> EA][C <sub>18</sub> OO]	0.0	0.0075	0.73	0.9980	0.0032 ± 0.00002 aA
[H <sub>2</sub> EA][C <sub>18:1</sub> OO]	0.0	0.0011	1.00	0.9982	0.0019 ± 0.00001 bA
[Ch][C <sub>18</sub> OO]	0.0	0.0065	0.77	0.9985	0.0033 ± 0.00002 aB

156  $^{\ddagger}k$  and  $^{\dagger}n$  for Herschel-Bulkley model.  $\eta$  is the apparent viscosity.

157 **References**

158 1. T. J. Mason, J. P. Lorimer, D. M. Bates and Y. Zhao, *Ultrasonics Sonochemistry*, 1994, **1**, S91-S95.

159

160